ChemComm

# Threefold Reactivity of a COF-Embedded Rhenium Catalyst: Reductive Etherification, Oxidative Esterification or Transfer Hydrogenation



| | |
|---|---|
| Journal: | *ChemComm* |
| Manuscript ID | CC-COM-06-2022-003173.R1 |
| Article Type: | Communication |
| | |

COMMUNICATION

# Threefold Reactivity of a COF-Embedded Rhenium Catalyst: Reductive Etherification, Oxidative Esterification or Transfer Hydrogenation

Received 00th January 20xx,
Accepted 00th January 20xx

DOI: 10.1039/x0xx00000x

Sean T. Goralski[b], Krystal M. Cid-Seara[a], Jenni J. Jarju[a], Laura Rodriguez-Lorenzo[a], Alec P. LaGrow[a], Michael J. Rose[b]* and Laura M. Salonen[a,c]*

**The reactivity of the novel Re(I) catalyst [Re($^{C12}$Anth-py$_2$)(CO)$_3$Br] is modulated by its interactions with the covalent organic framework (COF) TFB-BD. The complex catalyzes either reductive etherification, oxidative esterification, or transfer hydrogenation depending on its local environment (embedded in TFB-BD, in homogeneous solution, or co-incubated with TFB-BD respectively). The results highlight that COFs can drastically modulate the reactivity of homogeneous catalysts.**

The reactivity and selectivity of catalytic sites — whether molecular, biochemical or heterogeneous — has been historically ascribed to the atoms directly involved in the bond-making and bond-breaking events. However, the effect of secondary interactions and confined spaces in modulating reactivity and selectivity has become evident in recent years. Non-covalent immobilization of molecular catalysts in porous materials is a promising design strategy for new heterogeneous catalysts to attain enhanced reactivity and selectivity. This approach produces uniform and tunable catalytic environments that are unavailable to homogeneous catalysts.[1]

Like enzymes, catalytic pockets of porous materials may provide favorable intermolecular interactions and complementary close contacts between the active site and the substrates; thus, such environments use spatial confinement to adjust selectivity and reactivity. Covalent organic frameworks (COFs) are a class of porous, crystalline materials composed of organic building blocks connected by covalent bonds; these materials can be prepared with precise control over composition and topology.[2] The high surface area of a COF and its customizable pore size, shape and environment render this class of materials as promising candidates for heterogeneous catalysis.[3,4] Several strategies have been reported to develop COF materials for catalysis, including (*i*) incorporation of catalytic sites into the COF building blocks,[5-7] (*ii*) post-synthetic metal coordination by the pore wall,[8,9] (*iii*) integration of a pre-assembled molecular catalyst via post-synthetic reactions,[10] (*iv*) confinement of metal nanoparticles[11-13] or complexes[45] within the pores, and (*v*) insertion of polymers to provide cooperative catalytic sites.[14,15]

One well-known metal-catalyzed reaction of recent importance is transfer hydrogenation (TH) in both biomimetic and synthetic schemes. In this vein, *N,N*-chelated manganese(I) tricarbonyl complexes have garnered much attention in the literature for their TH reactivity.[16] Rhenium(I) congeners of such catalysts are attractive synthetic targets as they provide greater thermal and chemical stability for a wider range of catalytic systems. Such rhenium complexes featuring the same *N,N*-chelated rhenium(I) tricarbonyl motif have found their most notable application as catalysts for non-aqueous reduction of $CO_2$ to CO by both electrochemical[17-20] and photochemical[21,22] means. However, to our knowledge, application of this class of rhenium complexes to TH catalysis has not been reported, although Re–H species have been spectroscopically and structurally characterized[23] and phosphine-based Re(I/III) systems have been reported to catalyze TH catalysis.[24]

In this work, we demonstrate that the molecular catalyst [Re($^{C12}$Anth-py$_2$)(CO)$_3$Br] exhibits vastly different product outcomes dependent on the presence or absence of a single heterogeneous 'partner'. Remarkably, embedding our rhenium complex in the COF generates a hybrid heterogeneous catalyst, which provides unexpected reductive etherification (aldehyde→ester→ether) in a single reaction. Meanwhile, the isolated molecular catalyst *in homogeneous solution* exhibits only the aldehyde→ester transformation (oxidative esterification) — without further reduction to the ether. Furthermore, the same catalyst co-incubated with the COF support (but not embedded) exhibits the initially expected transfer hydrogenation. We thus emphasize the utility of COF materials to achieve varying reactivity using only *non-covalent* interactions with a molecular catalyst. Such a simple and tunable approach promises a greater scope of catalytic outcomes with existing materials without further catalyst development.

The catalyst [Re($^{C12}$Anth-py$_2$)(CO)$_3$Br] was synthesized according to an analogous procedure previously reported by us (without a dodecyl chain)[19]. The synthesis included a first step of alkylating 4,5-dichloroanthracene-9(10*H*)-one with 1-bromododecane via Grignard addition, thus obtaining the 1,8-dichloro-9-dodecylanthracene scaffold used for Suzuki coupling to the pyridine moieties. The addition of a dodecyl chain to the ligand scaffold was twofold important: *i*) iminic COFs related to TFB-BD are known to effectively sequester nonpolar species like hydrocarbons and small molecule drugs from aqueous solution, thus we aimed to increase the stability of the COF|molecule hybrid;[42,43] and *ii*) the 9-dodecylanthracene scaffold exhibits enhanced solubility compared to the unmodified anthracene scaffold, and this property was hypothesized to facilitate the catalyst embedding procedure. As target crystalline material to

[a] Department of Chemistry, University of Texas at Austin, 105 E. 24th St. Stop A5300, Austin, TX 78712, USA
[b] International Iberian Nanotechnology Laboratory (INL), Av. Mestre José Veiga, 4715-330, Braga, Portugal
[c] CINBIO, Universidade de Vigo, Department of Organic Chemistry, 36310 Vigo, Spain
*Corresponding authors

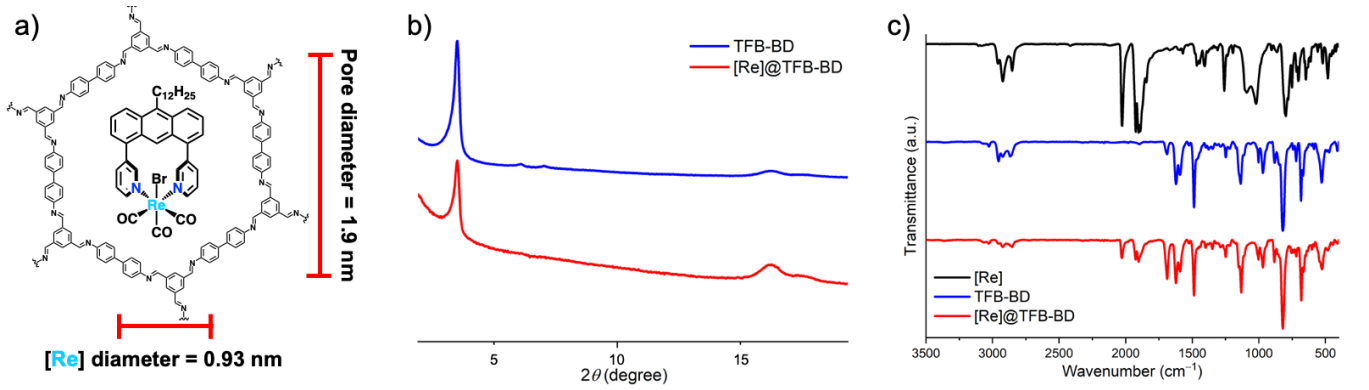


**Figure 1.** (a) The molecular structure of one pore of [Re]@TFB-BD; (b) powder XRD pattern of TFB-BD (*blue*) and [Re]@TFB-BD (*red*); (c) FTIR spectra of ($^{C12}$Anth-py$_2$)Re(CO)$_3$Br (*black*), TFB-BD (*blue*) and [Re]@TFB-BD (*red*).

enable full characterization, we chose the complementary COF material TFB-BD (*vide infra*), which features a pore size of ~2 nm (20 Å)[25] that is suitable to incorporate the 1 nm diameter of [Re($^{C12}$Anth-py$_2$)(CO)$_3$Br]. The BD building block lining the COF pores was envisioned to provide suitable hydrophobic interactions with the anthracene moiety and the alkyl tail. The structure is formed by the self-assembly of 1,3,5-triformylbenzene (TFB) and 1,1'-biphenyl-4,4'-diamine (BD) (**Figure 1a**). Imine-based COFs — as compared with those linked by boronic ester[26] — feature enhanced stability against hydrolysis.

A literature procedure[25] was adapted to prepare TFB-BD (COF) using TFB and BD in a ratio of 1:1.5 heated in a mixture of mesitylene and 1,4-dioxane (1:1) with aqueous 6 M acetic acid as catalyst at 120 °C for 3 days, thus providing a crystalline product. The small-angle X-ray diffraction (SAXS) pattern exhibited reflections at $2\theta$ = 3.5, 6.1, 7.1 and 16.2° (**Figure 1b**), consistent with the literature report.[38] COF formation was further supported by the Fourier-transform infrared (FTIR) spectrum that exhibited a feature at 1623 cm$^{-1}$ corresponding to the C=N stretch, similar to the reported data[38] (**Figure 1c**). The accessible surface area of TFB-BD was examined by $N_2$ sorption measurement at 77 K, evidencing a type I isotherm (**Figure S1**) that is typical of microporous materials. The BET surface area of TFB-BD was 847 m$^2$ g$^{-1}$, and the pore size distribution calculated using the QSDFT model for slit/cylindrical pores (adsorption branch) showed a maximum at 1.5 nm (**Figure S1–S2**) also in agreement with literature.[25]

To embed the rhenium catalyst in this COF, TFB-BD (155 mg) was treated with a $CH_2Cl_2$ solution of [Re($^{C12}$Anth-py$_2$)(CO)$_3$Br] (7 mg) and then the solid dried at 90 °C under $N_2$ atmosphere (ambient pressure) for 48 h to obtain [Re]@TFB-BD (~1% Re by atomic mass). Powder XRD confirmed that the crystallinity of [Re]@TFB-BD (**Figure 1b**) with the sharp reflection at $2\theta$ = 3.5° was preserved. FTIR spectroscopy evidenced both the preservation of the pristine TFB-BD spectrum *and* the appearance of new features at 2028, 1926, and 1902 cm$^{-1}$ — corresponding to the Re(C≡O)$_3$ moiety of [Re($^{C12}$Anth-py$_2$)(CO)$_3$Br] (**Figure 1c**).

Comparison of the Raman spectra of pristine TFB-BD and [Re]@TFB-BD (**Figure S6**) evidenced the vibrational modes observed for [Re($^{C12}$Anth-py$_2$)(CO)$_3$Br] invisible or largely shifted in the spectrum of [Re]@TFB-BD. The new features at 208 and 1013 cm$^{-1}$ and the increase in the intensity of the bands at 785 and 1215 cm$^{-1}$ in the spectrum of [Re]@TFB-BD could be assigned to Re–Br stretching, ring deformations, and C–N and C–C stretching from the catalyst.[39] A slight red-shift was observed for the COF features centered at 1584 cm$^{-1}$ and 1170 cm$^{-1}$ ($\Delta_{Raman\text{-}shift}$ = 2–4 cm$^{-1}$), accompanied by a slight increase in the broadness (FWHM) for TFB-BD is 30 cm$^{-1}$, while for [Re]@TFB-BD is 34 cm$^{-1}$) (**Figure S7**). These features may originate from structural distortions of the COF crystal in the presence of [Re($^{C12}$Anth-py$_2$)(CO)$_3$Br], which supports the hypothesis of the catalyst occupying the COF pores. Such shifts in the positions of the Raman features have been reported for metal–organic frameworks (MOF, e.g. Mn-MOF-74 or Co-MOF-74)[40,41] impregnated with small organic compounds (e.g. 7,7,8,8-tetracyanoquinodimethane).

The $N_2$ physisorption showed a decrease of the BET surface area by 53% down to 396 m$^2$ g$^{-1}$ upon [Re] incorporation, as expected for a molecular complex blocking the pores (**Figures S1, S4–S5**). Pore size distribution showed a maximum at 1.4 nm, nearly identical to the as-synthesized COF material. Thermogravimetric analysis (TGA) indicated material stability up to 380 °C, similar to the pristine COF (**Figures S8–S9**). High-angle annular dark field–scanning transmission electron microscopy (HAADF–STEM) of [Re]@TFB-BD evidenced single atom Re as bright dots on the COF support (**Figure S10**), and energy dispersive X-ray spectroscopy maps in STEM (STEM–EDX) indicated that the Re sites were evenly distributed throughout the COF material (**Figure S11**).

Upon substantiating the composition of [Re]@TFB-BD, we next investigated the transfer hydrogenation activity of the hybrid material with $^i$PrOH and acetophenone. In a closed reaction vessel, 1 equiv acetophenone was heated to 70 °C with 7.0 mg of [Re]@TFB-BD and 5 mol% of potassium *tert*-butoxide (KO$^t$Bu) in $^i$PrOH, which serves as both solvent and sacrificial hydrogen ($H_2$) donor. After 48 h, GCMS analysis indicated no reaction had occurred and only acetophenone (starting material) was observed. In contrast, the same reaction with benzaldehyde provided 59% conversion (GCMS) of benzaldehyde to benzyl isopropylether *with no side products* (**Figure S12**) — rather than the expected transfer hydrogenation product (benzyl alcohol). In the negative control reaction, no reaction was observed using *unmodified* TFB-BD under the same reaction conditions. Furthermore, no leaching of the Re($^{C12}$Anth-py$_2$) (CO)$_3$Br catalyst into the $^i$PrOH solution was detected by $^1$H NMR, FTIR spectroscopy or GCMS (*vide infra*, co-incubation study).

To determine the role of the TFB-BD scaffold in this unexpected catalytic transformation, we explored the reactivity of homogeneous [Re($^{C12}$Anth-py$_2$)(CO)$_3$Br] in the *absence* of COF. The analogous reaction performed with benzaldehyde [1 equiv, 5 mol% [Re($^{C12}$Anth-py$_2$)(CO)$_3$Br], 5 mol% of KO$^t$Bu in $^i$PrOH] resulted in 97% conversion from the starting material to products (GCMS). However, rather than the reduced benzyl isopropylether product observed in

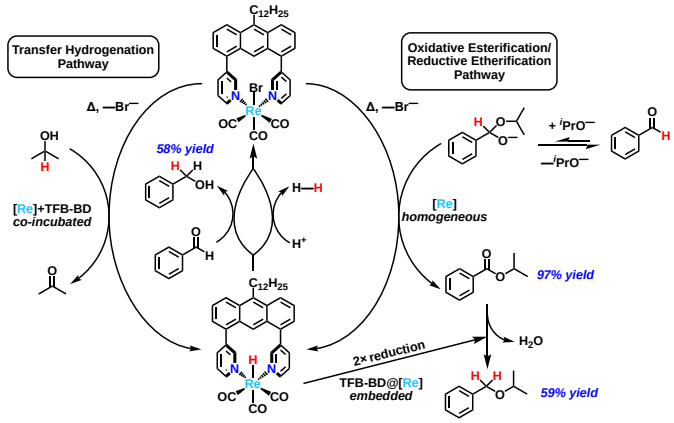


**Figure 2** Proposed catalytic cycles for the transfer hydrogenation (left) and oxidative esterification/reductive etherification (right) of benzaldehyde by [Re($^{C12}$Anth-py$_2$)(CO)$_3$Br].

the hybrid [Re]@TFB-BD catalyst system, we instead observed the *oxidative esterification* of benzaldehyde to isopropyl benzoate with no side products (**Figure S13**). On this basis, we conclude that the alteration in reactivity resulted from immobilization of the rhenium catalyst in the TFB-BD pores.

This finding enters [Re($^{C12}$Anth-py$_2$)(CO)$_3$Br] into a limited group of catalysts that perform oxidative esterification of aldehydes. The direct catalytic conversion of aldehydes to esters is step-efficient and atom-economic compared with the canonical reaction sequence of aldehyde oxidation followed by alcohol condensation. There are limited reports of transition metal catalysts that mediate this transformation. Furthermore, the utility and scalability of such methods is hindered by the need for high temperature and pressure,[27] co-catalysts,[28-30] or stoichiometric oxidizing agents.[31,32] Notably, metal-free methods for the oxidative esterification of aldehydes[33-35] remain limited by stoichiometric oxidants.

To demonstrate a host-guest interaction in the [Re]@TFB-BD ensemble, another set of reactions was performed using the rhenium catalyst simply co-incubated with (but not embedded within) TFB-BD. That is, [Re($^{C12}$Anth-py$_2$)(CO)$_3$Br] was dissolved in $^{i}$PrOH and *pristine* (unmodified) TFB-BD was suspended therewith. Benzaldehyde was then heated with this mixture under the same conditions ($^{i}$PrOH 70 °C, 5 mol% catalyst, 5 mol% KO$^{t}$Bu). We hypothesized that oxidative esterification would proceed as in the homogeneous reaction (with no added TFB-BD), as the evaporative embedding procedure was not followed. Unexpectedly, the reaction generated neither the oxidative esterification product (isopropyl benzoate) *nor* the reduction product (benzyl isopropylether), but instead a new set of products: 58% conversion of benzaldehyde to benzyl alcohol (22%), benzalacetone (7%), and dibenzalacetone (29%) in a ~3:1:4 ratio. Indeed, these products are the result of the *initially hypothesized* rhenium-mediated transfer hydrogenation, which produces benzyl alcohol and 1 equiv of acetone. Subsequently, the byproduct acetone undergoes aldol condensation with unreacted benzaldehyde either once to afford benzalacetone, or twice to afford dibenzalacetone. The same reaction performed in the *absence* of KO$^{t}$Bu still provides transfer hydrogenation, but (beneficially) no aldol condensation side products are observed (benzyl alcohol 55%).

Overall, we sought to propose a mechanism for the various reaction pathways observed in the [Re]±TFB-BD systems described above. Considering the homogeneous system ([Re] without TFB-BD) that performed oxidative esterification, we desired to determine if a Re(I) hydride species was formed in the reaction. Formation of Re–H would likely result from the oxidation of benzaldehyde-isopropanol hemiacetal, as this species would be far more hydridic than benzaldehyde. (Notably, neither the reductive etherification nor the oxidative esterification occurs in the absence of KO$^{t}$Bu base.) Thus, the oxidative esterification reaction (as described earlier) was performed in a sealed NMR tube using $d_8$-isopropanol. The $^{1}$H NMR spectrum of the mixture after 18 h exhibited a resonance at –5.45 ppm (**Figure S16**), indicating the presence of a bridged Re–H–Re species.[37] This dimeric species was then generated *ex situ* by reaction of [Re($^{C12}$Anth-py$_2$)(CO)$_3$(solv)]$^{+}$ (via AgBF$_4$) with NaBH$_4$,[36] which afforded the same bridged hydride species (δ –5.34 ppm, $^{1}$H NMR) as the major product, with a small amount of terminal Re–H product (δ –17.2 ppm, $^{1}$H NMR; 15:1 bridged:terminal ratio). This chemical shift is in good agreement with a previously reported analogous compound [(μ-H)(Re(bpy)(CO)$_3$)$_2$].[36] Since the only hydride donor (as opposed to deuteride donor) in the solution is the benzaldehyde substrate, we conclude that oxidative esterification occurs by Re-mediated hydride abstraction from the hemiacetal of benzaldehyde (**Figure 2**).

Next, examining the [Re]@TFB-BD hybrid system: a homogeneous system was reported wherein a manganese(I) tricarbonyl reduced esters to ethers via manganese-mediated hydride transfer.[37] We propose that ether formation in the [Re]@TFB-BD system occurs by oxidative esterification and subsequent reduction by the embedded Re–H species to afford the ether product (**Figure 2**). We propose that this second step (reduction) occurs only in the hybrid catalyst system (and not in the homogeneous system) because the catalytic sites are co-immobilized in the pores of TFB-BD with trapped substrate. This immobilization serves (*i*) to stabilize the *terminal* Re–H intermediate and prevent the catalyst-inactivating formation of Re–H–Re, and (*ii*) to trap the ester intermediate in close proximity to the reactive Re–H species, thus promoting reduction. To test this hypothesis, *ex situ*-prepared isopropyl benzoate was reacted with [Re]@TFB-BD, and its reduction to benzyl isopropyl ether was observed (**Figure S18**).

Finally, we consider the system of [Re($^{C12}$Anth-py$_2$)(CO)$_3$Br] co-incubated with TFB-BD. As a Re(I)–H intermediate (δ –5.34 ppm) was observed in the (completely) homogeneous catalytic system, we postulate that the TH activity observed in this system follows the reported mechanism of Mn(I)–H transfer hydrogenations.[16,38] Notably, the reported manganese systems utilize a pendant base moiety (such as 2-hydroxypyridine) for effective catalysis, as the pendant base acts as a proton acceptor/donor. As such, our *pyridine*-based rhenium complex cannot efficiently catalyze TH in the absence of a proximal pendant base. It is thus possible that the aryl-NH$_2$ groups at the TFB-BD termini act as such a pendant base in the present system, leading to TH activity. Additionally, adsorption of [Re($^{C12}$Anth-py$_2$)(CO)$_3$Br] to the surface of TFB-BD would result in close spatial proximity of the rhenium center to the amino termini. It has been observed in metal organic framework (MOF) catalytic systems that the MOF scaffold can provide important secondary interactions to catalytic sites which alter and enhance reactivity.[44]

## Conclusions

This work demonstrates that the presence and mode of interaction (embedded or co-incubated) of a COF co-catalyst drastically alters the reactivity of a homogeneous rhenium catalyst, which determines its varying functional outcome: reductive etherification (COF-embedded catalyst), oxidative esterification (homogeneous catalyst) and transfer hydrogenation (co-incubated catalyst). This demonstrates the utility of COF materials to maintain their crystalline structure whilst altering the inherent reactivity of molecular species

— *even in the absence of covalent tethering*. Such a hybrid material|catalyst strategy is a practical and tractable approach for developing of new catalytic systems based on known catalysts.

**Acknowledgement.** The authors acknowledge the financial support from the COFforH2 project (UTA-EXPL/NPN/0055/2019) through the Portuguese Foundation for Science and Technology – FCT funds under UT Austin Portugal. L.R.-L. acknowledges funding to FCT (Fundação para a Ciência e Technologia) for the Scientific Employment Stimulus Program (2020.04021.CEECIND). We thank the Nanophotonics & Bioimagins and the Advanced Electron Microscopy, Imaging & Spectroscopy (AEMIS) facilities and staff at INL for contributions to this publication. MJR acknowledges the Welch Foundation (F-1822). LMS acknowledges financial support from the Spanish Ministry of Science through the Ramón y Cajal grant RYC2020-030414-I.

## Conflicts of interest

There are no conflicts to declare.

## Notes and references

1 X. Wang, F. M. Wisser, J. Ø, M. Fontecave and C. Mellot-draznieks, *ChemSusChem*, 2018, **11**, 3315–3322.
2 C. Qian, W. Zhou, J. Qiao, D. Wang, X. Li, W. L. Teo, X. Shi, H. Wu, J. Di, H. Wang, G. Liu, L. Gu, J. Liu, L. Feng, Y. Liu, S. Y. Quek, K. P. Loh and Y. Zhao, *J. Am. Chem. Soc.*, 2020, **142**, 18138–18149.
3 J. Guo and D. Jiang, *ACS Cent. Sci.*, 2020, **6**, 869–879.
4 S. T. Emmerling, F. Ziegler, F. R. Fischer, R. Schoch, M. Bauer, B. Plietker, M. R. Buchmeiser and B. V. Lotsch, *Chem. - Eur. J.*, DOI:10.1002/chem.202104108.
5 Y. Yue, P. Cai, K. Xu, H. Li, H. Chen, H. Zhou and N. Huang, *J. Am. Chem. Soc.*, 2021, **143**, 18052–18060.
6 S. Lin, C. S. Diercks, Y. Zhang, N. Kornienko, O. M. Yaghi and C. J. Chang, *Science* 2015, **349**, 33–37.
7 J. J. Jarju, A. M. Díez, L. Frey, V. Sousa, E. Carbó-Argibay, D. D. Medina, O. I. Lebedev, Yu. V. Kolen'ko, L. M. Salonen, *under review*.
8 W. Zhong, R. Sa, L. Li, Y. He, L. Li, J. Bi, Z. Zhuang, Y. Yu and Z. Zou, *J. Am. Chem. Soc.*, 2019, **141**, 7615–7621.
9 X. Han, Q. Xia, J. Huang, Y. Liu, C. Tan and Y. Cui, *J. Am. Chem. Soc.*, 2017, **139**, 8693–8697.
10 S. I. Hong Xu, Xiong Chen, Jia Gao, Jianbin Lin, Matthew Addicoat and D. J. Jiang, *Chem. Commun.*, 2014, **50**, 1292–1295.
11 S. Ghosh, T. S. Khan, A. Ghosh, A. H. Chowdhury, M. A. Haider, A. Khan and S. M. Islam, *ACS Sustain. Chem. Eng.*, 2020, **8**, 5495–5513.
12 W. Hao, D. Chen, Y. Li, Z. Yang, G. Xing, J. Li and L. Chen, *Chem. Mater.*, 2019, **31**, 8100–8105.
13 L. P. L. Gonçalves, D. B. Christensen, M. Meledina, L. M. Salonen, D. Y. Petrovykh, J. P. S. Sousa, O. Salomé, G. P. Soares, E. Carbó-Argibay, M. Fernando R., Pereira, S. Kegnæs, Y. V. Kolen'ko, ***Catal. Sci. Technol.***, 2020, **10**, 1991-1995.
14 Q. Sun, B. Aguila, J. Perman, N. Nguyen and S. Ma, *J. Am. Chem. Soc.*, 2016, **138**, 15790–15796.
15 Q. Sun, Y. Tang, B. Aguila, S. Wang, F. S. Xiao, P. K. Thallapally, A. M. Al-Enizi, A. Nafady and S. Ma, *Angew. Chem. Int. Ed.*, 2019, **58**, 8670–8675.
16 K. Das, M. K. Barman and B. Maji, *Chem. Commun.*, 2021, **57**, 8534-8549.
17 J. Hawecker, J. M. Lehn and R. Ziessel, *J. Chem. Soc. Chem Commun.*, 1984, 328-330.
18 J. A. Keith, K. A. Grice, C. P. Kubiak and E. A. Carter, *J. Am. Chem. Soc.* 2013, **135**, 15823-15829.
19 T. A. Manes and M. J. Rose, *Inorg. Chem. Comm.*, 2015, **61**, 221-224.
20 S. Oh, J. R. Gallagher, J. T. Miller and Y. Surendranath, *J. Am. Chem. Soc.*, 2016, **138**, 6, 1820-1823.
21 J. Hawecker, J. M. Lehn and R. Ziessel, *J. Chem. Soc. Chem. Commun.*, 1983, 536-538.
22 J. Ettedgui, Y. Diskin-Posner, L. Weiner and R. Neumann, *J. Am. Chem. Soc.*, 2011, **133**, 188-190.
23 G. Cianai, A. Sironi, G. D'Alfonso, P. Romiti, M. Freni and *J. Organometallic Chem.*, 1983, **254**, 3, C37-C41.
24 Y. Jiang, O. Blacque, T. Fox, C. M. Frech and B. Heinz, *Organometallics*, 2009, **28**, 18, 5493-5504.
25 Q. Gao, L. Bai, Y. Zeng, P. Wang, X. Zhang, R. Zou and Y. Zhao, *Chem. Eur. J.*, 2015, **21**, 16818–16822.
26 L. Frey, J. J. Jarju, L. M. Salonen and D. D. Medina, *New J. Chem.*, 2021, **45**, 14879-14907.
27 S. Murahasgi, T. Naota, K. Ito, Y. Maeda and H. Taki, *J. Org. Chem.*, 1987, **52**, 4319-4327.
28 W. Yoo and C. Li, *Tetrahedron Lett.*, 2007, **48**, 1033-1035.
29 N. Yamamoto, Y. Obora and Y. Ishii, *J. Org. Chem.*, 2011, **76**, 2937-2941.
30 C. Liu, S. Tang, L. Zheng, D. Liu, H. Zhang and A. Lei, *Angew. Chem. Int. Ed.*, 2012, **51**, 5662-5666.
31 R. Gopinath, B. K. Patel, *Org. Lett.*, 2000, **2**, 577-579.
32 F. F. Arp, R. Ashirov, M. Bhuvanesh and J. Blümel, *Dalton Trans.*, 2021, **42**, 15296-15309.
33 B. R. Travis, M. Sivakumar, G. O. Hollist and B. Borhan, *Org. Lett.* 2003, **5**, 1031-1034.
34 N. T. Reynolds, J. R. de Alaniz and T. Rovis, *J. Am. Chem. Soc.*, 2004, **126**, 9518-9519.
35 X. Luo, D. Ge, Z. Yu, X. Chu and P. Xu, *RSC Adv.*, 2021, **11**, 30937-30942.
36 J. Hawecker, J. M. Lehn and R. Ziessel, *Helv. Chim. Acta*., 1986, **69**, 8, 1990-2012.
37 O. Martinez-Ferrate, B. Chatterjee, C. Werle and W. Leitner, *Catal. Sci. Technol.*, 2019, **9**, 22, 6370-6378.
38 A. Dubey, S. M. Wahidur Rhaman, R. R. Fayzullin and J. R. Khusnutdinova, *ChemCatChem*., 2019, **11**, 3844-3852.
39 M. Pižl, A. Picchiotti, M. Rebarz, N. Lenngren, L. Yingliang, S. Záliš, M. Kloz and A Vlček, *J. Phys. Chem. A.*, 2020, **124**, 7, 1253-1265.
40 M. Bláha, V. Valeš, Z. Bastl, M. Kalbáč, H. Shiozawa, *J. Phys. Chem. C.*, 2020, **124**, 44, 24245-24250.
41 H. Shiozawa, B. C. Bayer, H. Peterlik, J. C. Meyer, W. Lang and T. Pichler, *Sci. Rep.*, 2017, **7**, 2439.
42 S. P. S. Fernandes, V. Romero, B. Espiña, L. M. Salonen, *Chem. Eur. J.*, 2019, **25**, 6461-6473.
43 A. Mellah, S. P. S. Fernandes, R. Rodríguez, J. Otero, J. Paz, J. Cruces, D. D. Medina, H. Djamila, B. Espiña, L. M. Salonen, *Chem. Eur. J.*, 2018, **24**, 10601-10605.
44 K. Hemmer, M. Kokoja, R. A. Fischer, *ChemCatChem*, 2021, **13**, 1683-1691.
45 H. S. Sasmal, S. Bag, B. Chandra, Majumder, H. Kuiry, S. Karak, S. S. Gupta, R. Banerjee, *J. Am. Chem. Soc.*, 2021, **143**, 8426-8436.

 